Broadly heterogeneous activation of the master regulator for sporulation in Bacillus subtilis

Arnaud Chastanet, Dennis Vitkup, Guo-Cheng Yuan, Thomas M Norman, Jun S Liu, Richard M Losick

HAL Id: hal-02667835
https://hal.inrae.fr/hal-02667835v1

Submitted on 31 May 2020

Broadly heterogeneous activation of the master regulator for sporulation in *Bacillus subtilis*

Arnaud Chastanet[a,1], Dennis Vitkup[b,2], Guo-Cheng Yuan[c], Thomas M. Norman[a], Jun S. Liu[d], and Richard M. Losick[a,2]

[a]Department of Molecular and Cellular Biology, Harvard University, Cambridge, MA 02138; [b]Center for Computational Biology and Bioinformatics, Department of Biomedical Informatics, Columbia University, New York, NY 10032; [c]Department of Biostatistics and Computational Biology, Dana-Farber Cancer Institute, Harvard School of Public Health, Boston, MA 02115; and [d]Department of Statistics, Harvard University, Cambridge, MA 02138

A model system for investigating how developmental regulatory networks determine cell fate is spore formation in *Bacillus subtilis*. The master regulator for sporulation is Spo0A, which is activated by phosphorylation via a phosphorelay that is subject to three positive feedback loops. The ultimate decision to sporulate is, however, stochastic in that only a portion of the population sporulates even under optimal conditions. It was previously assumed that activation of Spo0A and hence entry into sporulation is subject to a bistable switch mediated by one or more feedback loops. Here we reinvestigate the basis for bimodality in sporulation. We show that none of the feedback loops is rate limiting for the synthesis and phosphorylation of Spo0A. Instead, the loops ensure a just-in-time supply of relay components for rising levels of phosphorylated Spo0A, with phosphate flux through the relay being limiting for Spo0A activation and sporulation. In addition, genes under Spo0A control did not exhibit a bimodal pattern of expression as expected for a bistable switch. In contrast, we observed a highly heterogeneous pattern of Spo0A activation that increased in a nonlinear manner with time. We present a computational model for the nonlinear increase and propose that the phosphorelay is a noise generator and that only cells that attain a threshold level of phosphorylated Spo0A sporulate.

noise | Spo0A | bistable switch | cell fate | heterogeneity

A challenge in developmental biology is to understand how cells in an apparently homogeneous population adopt different fates. An attractive organism in which to address this challenge is *Bacillus subtilis*, which can adopt a variety of alternative fates depending on growth conditions (1–3). In some cases, cell population heterogeneity is generated stochastically. That is, fluctuations in gene expression due to noise can be amplified by feedback loops to lock cells in alternative stable states, resulting in a bimodal distribution of cell types. This is exemplified by genetic competence in which a positive feedback loop acting as a bistable switch creates such a distribution (2, 4). We use *bimodal* to mean systems that exhibit two discrete states and *bistable* to specify a class of bimodal systems in which nonlinear reinforcement stabilizes the alternative states. Here we are concerned with bimodality in the capacity of *B. subtilis* to sporulate.

The master regulator for entry into sporulation, Spo0A (0A), accumulates gradually over the first 90 min of sporulation (5) (Fig. S1.) and is only active in its phosphorylated form (0A~P) (6). Some genes under its control, such as those involved in biofilm formation and cannibalism, have strong binding sites for 0A~P and are switched ON at low levels of 0A~P. Other genes, such as those for spore formation, have weak binding sites and are only activated when 0A~P accumulates to high levels (5, 7). The accumulation of 0A~P is governed by a regulatory network built around a four-component cascade in which the relay protein Spo0F (0F) is phosphorylated by KinA and other kinases (6, 8). 0F~P, in turn, transfers the phosphate to Spo0B (0B), which transfers the phosphate to 0A (Fig. 1A).

At least four feedback loops impinge on the relay. First, 0A~P stimulates the transcription of its own gene (*spo0A*), acting at a promoter P_s that is recognized by RNA polymerase containing σ^H. Second, 0A~P stimulates the transcription of the gene (*spo0F*) for 0F. Third, 0A~P represses the gene (*abrB*) for AbrB, which in turn represses the transcription of the gene (*sigH*) for σ^H. Finally, 0A~P, via repression of *abrB*, derepresses the gene (*spo0E*) for a 0A~P-specific phosphatase Spo0E (0E). The first two pathways (0A~P→ *spo0A*; 0A~P→ *spo0F*) are simple positive feedback loops. The third (0A~P⊣ *abrB* ⊣ *sigH*) is also a positive feedback loop in that σ^H directs transcription of *kinA*, *spo0A*, and *spo0F*. Finally, the fourth pathway (0A~P⊣ *abrB*⊣ *spo0E*) is a negative feedback loop in that 0E drains phosphates from the relay (for review see ref. 8).

A striking feature of sporulation is its dichotomy: even under optimal conditions only a portion of the population forms spores (9). The decision of whether to sporulate is dictated by the accumulation of 0A~P. Thus, a tempting hypothesis to explain the bimodality of sporulation was that distribution of 0A~P is itself bimodal because it is subject to a bistable switch (2, 10). The three positive feedback loops governing the synthesis and phosphorylation of 0A were attractive candidates for such a switch.

Here we have revisited the circuitry governing 0A synthesis and phosphorylation. We report that none of the positive feedback loops is rate limiting for the production of 0A. To the contrary, some of the loops seem to be just-in-time mechanisms. Moreover, we show that contrary to earlier thinking, 0A~P activity is not bimodal. Instead, the distribution of 0A~P levels among cells in the population is heterogeneous, with only those cells having a high threshold level of 0A~P going on to sporulate. Finally, we report that the accumulation of 0A~P, and hence the extent of sporulation, is primarily determined by the flux of phosphate through the relay. We propose that the relay is a noise generator and that this noisiness is responsible for the broadly heterogeneous accumulation of 0A~P. Thus, stochastic cell-to-cell variations in the level of 0A~P dictate whether to sporulate. Finally, we propose a computational model for the 0A regulatory network.

Results

Positive Feedback Loop Involving AbrB and σ^H Does Not Significantly Contribute to the Accumulation of 0A. First, we sought to systematically investigate the contribution of previously described reg-

Fig. 1. An intricate genetic circuitry controls 0A production and activation. (*A*) The network of feedback loops controlling 0A~P. Purple lines highlight the AbrB/σ^H pathway for transcription of the genes for KinA, 0F, and 0A. Orange lines highlight the AbrB/0E pathway promoting dephosphorylation of 0A~P. The blue and green lines identify positive feedback loops that stimulate transcription of the genes for 0A and 0F, respectively, via the accumulation of 0A~P. (*B*) A noise model for the generation of heterogeneity in 0A~P levels during sporulation. The 0A~P ⊣ AbrB → σ^H → 0A pathway is depicted in light gray because σ^H levels rise before sporulation starts. Because 0A and 0F levels are also not limiting, positive feedback loops governing their synthesis are "just-in-time" circuits (red) that maintain adequate supplies of both proteins as 0A~P levels rise. The 0E circuit (blue) imposes a time delay that impedes the accumulation of 0A~P at the start of sporulation. Finally, and most importantly, we propose that flux of phosphate through the relay is noisy and is responsible for the heterogeneity in 0A~P levels.

ulatory proteins to the accumulation of 0A, starting with AbrB and σ^H. Transcription of *abrB* is repressed by 0A~P, whereas AbrB, in turn, represses *spo0H*, the gene for σ^H (Fig. 1*A*). Finally, σ^H directs transcription of *spo0A*. Indeed, and consistent with earlier reports, the absence of AbrB led to a modest increase in σ^H levels during exponential phase growth (Fig. 2*A*). In contrast, the absence of 0A caused a marked increase in AbrB levels, resulting in the absence of σ^H. Thus, 0A, AbrB, and σ^H constitute a positive feedback loop.

To investigate whether this loop contributes to the accumulation of 0A at the start of sporulation (hour 0), we carried out the time course experiment shown in Fig. 2*A*. The results show that the accumulation of σ^H occurred in parallel with the induction of 0A synthesis and, importantly, that the reduction in AbrB levels commenced after 0A levels had already started to rise. Thus, the disappearance of AbrB could not be responsible for stimulating 0A synthesis. To further investigate the role of AbrB, we took advantage of the fact that *spo0A* is transcribed both from a vegetative promoter (P_v) responsible for 0A synthesis during growth (recognized by σ^A) and a σ^H-dependent promoter (P_s) required for sporulation (11). As expected, in a mutant lacking P_v, little or no 0A was present during growth, and, as a consequence, AbrB was at higher than normal levels at hour 0 and remained at high levels even at hour 2. Nonetheless, σ^H levels increased markedly between hours 0 and 2.

Finally, it is known that in addition to repressing *abrB*, 0A~P also turns on the synthesis of an antirepressor AbbA, which prevents AbrB from binding to DNA (12). However, our results show that AbbA is not responsible for derepression of *spo0H* and hence stimulation of 0A synthesis (Fig. S2). We therefore propose the following model (Fig. 2*C*): during early exponential phase in rich medium, AbrB is at its highest levels (13), thereby repressing its entire regulon. 0A~P begins to accumulate by midexponential phase, partially repressing *abrB*, allowing derepression of certain target genes, such as *spo0H*, with relatively low affinities for the repressor. Finally, after sporulation commences, 0A~P reaches higher levels, inducing AbbA synthesis and further derepression of AbrB targets. As a consequence, targets with high affinities for AbrB are derepressed.

0A~P but Not σ^H Is Rate Limiting for Accumulation of 0A. Little induction of the *lacZ* transcriptional fusion to *spo0H* (P_spo0H-*lacZ*) was seen at the same time that σ^H protein levels were rising (Fig. 2*A* and Fig. S2), indicating that accumulation of σ^H at hour 0 is controlled at a posttranscriptional level, as noted previously (14, 15). It therefore remained possible that σ^H is rate limiting for 0A synthesis and that the increase in σ^H contributes to the timing of induction of 0A synthesis. This possibility was ruled out by overproducing σ^H before the start of sporulation (Fig. S3*A*): despite the presence of high levels of σ^H by hour 0, the kinetics of

Fig. 2. The AbrB/σ^H pathway contributes negligibly to 0A~P accumulation. (*A*) Kinetics of accumulation of 0A, AbrB, and σ^H during sporulation. Blots were performed using samples of wild-type cells taken at the indicated times before and after suspension in sporulation-inducing synthetic minimal (SM) medium (*Right*) (25). Samples from cells mutant for *spo0A* (Δ0A; Abs549) and *abrB* (Δ*abrB*; RL3660) were taken immediately before suspension (*Left*). Equal amounts of protein, as quantified by the Bradford technique, were loaded as verified by the control immunoblot using anti-σ^A antibodies (*Top*). (*B*) σ^H accumulates to high levels even when AbrB levels remain high. Equivalent amounts of protein from wild type (wt) or mutant (mut; ΔP_veg*spo0A*) strains were loaded and analyzed using anti-0A, -σ^H, -AbrB, and -σ^A antibodies. (*C*) Model for the interplay of AbrB, AbbA, 0A~P, and σ^H from growth into sporulation. Arrow indicates transcriptional stimulation. Bars indicate repression or in the case of AbbA inhibition of AbrB protein. Font size conveys relative abundance of proteins. *Unknown posttranscriptional control of σ^H accumulation.

0A accumulation were unchanged. Next, we hypothesized that the increase in 0A synthesis could result from the feedback loop in which 0A~P stimulates transcription of its own gene. To investigate this, we asked whether the level of 0A~P would increase overall 0A protein levels. First, we observed that the absence of 0E (Fig. S3B), a phosphatase that dephosphorylates 0A~P, sped up the accumulation of 0A, but only modestly. However, using a strain that was both mutant for 0E and that overproduced one of the kinases in the phosphorelay [KinC (16)], we observed a dramatic acceleration of 0A accumulation, reducing the time required to reach maximum accumulation by 50% (Fig. S3B).

We then investigated the effect of increasing 0A~P levels on sporulation by monitoring asymmetric division, the commitment point that requires high levels of 0A~P. Wild-type cells with a polar septum began to appear at approximately hour 1, reaching a peak accumulation at hour 2 (Fig. 3A). The absence of 0E and the overproduction of either KinA or KinC markedly enhanced the rate of appearance of sporangia that had reached the stage of asymmetric division (Fig. 4B). Again, kinase overproduction, especially of KinC, had a more pronounced effect than did elimination of 0E. In addition, the proportion of cells with a polar septum reached almost 100%.

0A Protein Accumulation Is Not Rate Limiting. Because 0A~P stimulates the synthesis of 0A, the experiments shown in Fig. 3 did not distinguish between the possibility that 0A protein or phosphate flux through the relay was rate limiting. To discriminate between these alternatives, we took advantage of a *0A* mutant (*spo0A-up*) that is transcribed at higher than normal levels during exponential phase owing to the absence of a repressing element (to be described elsewhere). The immunoblot of Fig. 3B (*Inset*) shows that cells harboring *spo0A-up* entered sporulation with more 0A than did wild-type cells. Nonetheless, neither the rate nor the maximum fraction of sporulating cells was measurably higher than for the wild type. Similar results were obtained when 0A was overproduced using the inducible promoter P*spac* (Fig. 3C). We conclude that 0A protein is not rate limiting for sporulation.

Spo0F Is Not Rate Limiting. One final self-reinforcing cycle that could contribute to the accumulation of 0A~P is stimulation of *spo0F* transcription by 0A~P. To investigate this, we introduced a P*Hy-spo0F* fusion into the wild type or a *spo0F* null mutant and tested the effect of varying isopropyl ß-D-thiogalactoside (IPTG) concentrations. Whereas low concentrations of inducer stimulated sporulation in a *spo0F* mutant, high concentrations inhibited sporulation, possibly owing to the reported substrate inhibition of KinA-mediated phosphorylation at high 0F levels (17). Importantly, none of the tested concentrations supported sporulation at a higher efficiency than observed for the wild type (Fig. 3C). Finally, we considered the possibility that *spo0A* and *spo0F* would need to be up-regulated together to increase sporulation efficiency above that observed for the wild type. We therefore created a strain harboring both P*up-0A* and P*Hy-spo0F* and varied the concentration of IPTG. Again, at no concentration of inducer were we able to observe a higher level of sporulation than for the wild type (Fig. 3C).

Thus, neither 0A nor 0F nor σ[H] are rate limiting for sporulation. Instead, the evidence suggests that the rate-limiting step in the generation of 0A~P is the flux of phosphate through the phosphorelay. We therefore favor the view that the feedback loops governing 0A and 0F synthesis are just-in-time control circuits that are optimally tuned to the requirements of the system for rising levels of phosphorylated Spo0A.

0A Activity Is Broadly Heterogeneous. Next, because no feedback loop could account for the postulated bistable switch, we rein-
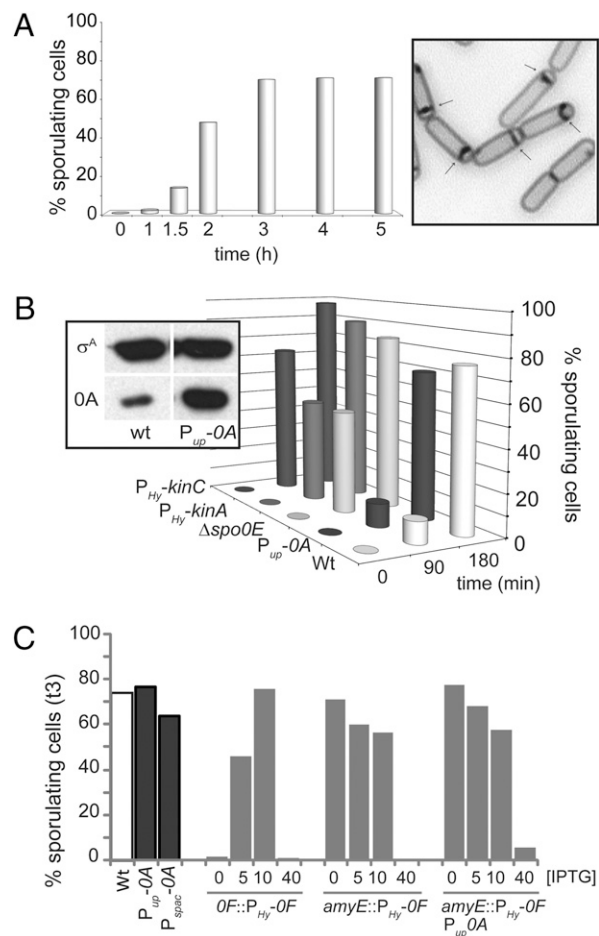

Fig. 3. Phosphate flux but not 0A or 0F levels is limiting for sporulation. (*A*) Sporulation was monitored by measuring the percentage of cells that had reached the stage of asymmetric division or beyond (*Inset:* arrows label asymmetric septa). Samples of wild-type cells suspended in synthetic minimal (SM) medium were collected, stained with Mito Tracker Green, and observed microscopically. A minimum of 500 cells was counted for each time point here and below. (*B*) Phosphate flux but not the initial level of 0A is limiting for sporulation. Sporulation was monitored as in *A* using wild-type (wt) cells, cells constitutively overexpressing *spo0A* because of a promoter up-mutation (P*up-0A*), cells mutant for *spo0E* (Δ*spo0E*; *spo0E::K$_m$*), cells overexpressing *kinA* (P*Hy-kinA*; *kinA::P$_{Hy}$-kinA*), or cells overexpressing *kinC* (P*Hy-kinC*; *kinC::P$_{Hy}$-kinC*). Expression of P*Hy-kinA* and P*Hy-kinC* were induced at the time of suspension in SM medium (time 0) by the addition of 1 mM (final concentration) IPTG. *Inset:* 0A levels were enhanced in the *spo0A* over-expression strain as measured by immunoblot analysis using anti-0A anti-bodies; samples of wild-type (wt) or P*up-0A* cells were collected at the time of suspension (time 0). Equal amounts of protein were analyzed as demonstrated with anti-σ[A] antibodies. (*C*) 0F levels are not limiting for sporulation. Sporulation was monitored as in *A* with wild-type (wt) cells, cells over-expressing *spo0A* with P*up-0A*, cells overexpressing *spo0A* with P*spac-0A*, cells overexpressing *spo0F* in a *spo0F* mutant background (*0F::P$_{Hy}$-0F*), cells overexpressing *spo0F* in *spo0F+* background (*amyE::P$_{Hy}$-0F*), and in cells overexpressing both *spo0A* and *spo0F* (P*up-0A*, *amyE::P$_{Hy}$-0F*). P*spac-0A* and P*Hy-0F* were induced 30 min before suspension by the addition of 1 mM IPTG (final concentration) for *spo0A*, or by a varying concentration of IPTG (numbers correspond to μM concentration) for *spo0F*.

vestigated the hypothesis that the distribution of 0A~P is bimodal (10). For this, we carried out fluorescence microscopy using a fusion of the gene for the GFP to the promoter (P*spoIIA*) for the 0A~P-controlled sporulation gene *spoIIA* (*IIA*). The results in Fig. 4A show that fluorescence was broadly heterogeneous, without clear indication of two distinct subpopulations. These results were confirmed by time-lapse flow cytometry,
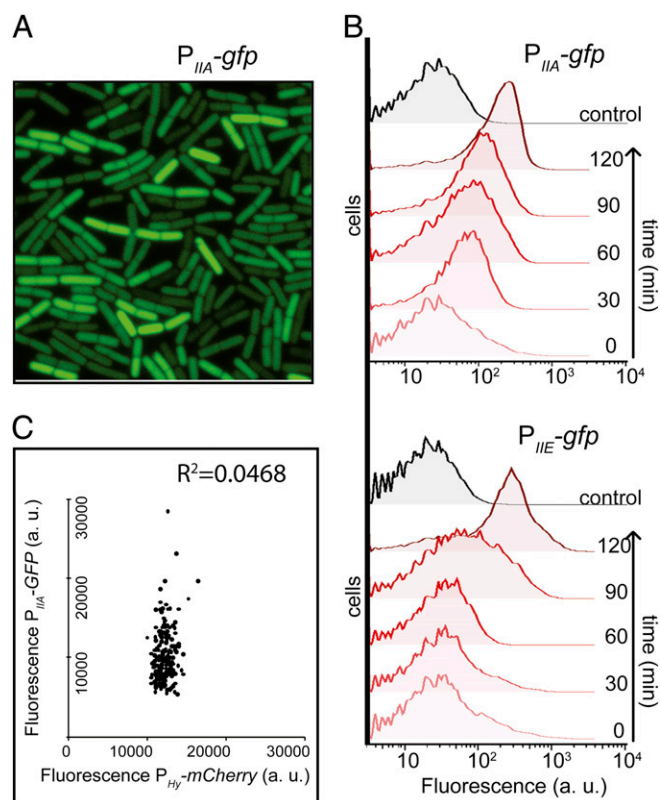
Fig. 4. 0A-directed gene expression is broadly heterogeneous. (*A*) Visualization of *amyE*::P*_IIA_*-*gfp* expression by fluorescence microscopy 1 h after induction of sporulation. (*B*) FACS analysis of cells harboring *amyE*::P*_IIA_*-*gfp* (*Upper*) or *amyE*::P*_IIE_*-*gfp* (*Lower*). The cells were grown in Casein Hydrolysate (CH) rich medium and suspended in SM medium at the midexponential phase of growth. Cells were collected at the indicated times after suspension and prepared for FACS analysis as described in *Materials and Methods*. The control (gray) was FACS analysis with wild-type cells lacking *gfp*. (*C*) Heterogeneity in a late 0A-target expression is uncorrelated with extrinsic noise. Green and red fluorescence were quantified in P*_IIA_*-*gfp* - P*_Hy_*-*mCherry* ABS1317 cells (*amyE*::P*_IIA_*-*gfp ylnF*::Tn*917*::*amyE*::*cat*::P*_Hy_*-*mCherry*). For this, *mcherry* was induced using a final concentration of 1 mM IPTG 1 h before induction for sporulation, and images were collected 90 min after sporulation induction. Average fluorescence intensity in individual cells was calculated on >500 cells using Metamorph software on a 10-pix² area replicated from "red" picture to "green" picture.

which revealed a gradual increase in the overall level of 0A~P-directed gene expression but without distinct subpopulations of cells (Figs. 4*B* and 5*A*).

That expression of P*_IIA_*-*gfp* was heterogeneous was verified by a double-label experiment using cells harboring P*_IIA_*-*gfp* and a fusion of an inducible promoter (P*_Hy_*) to the gene for mCherry (P*_Hy_*-*mCherry*). The result in Fig. 4*C* suggests that cell-to-cell expression levels for P*_IIA_*-*gfp* varied much more markedly than for P*_Hy_*-*mCherry*. Noisiness of *gfp* expression was confirmed by normalizing the data: indeed the coefficient of variation (CV, the ratio of the SD to its mean) of *mCherry* expression was less (0.103) than that of *gfp* (0.353). Furthermore, the low correlation coefficient between the levels of expression of the two fusions ($R^2 < 0.05$) indicates that their expression levels varied independently in each cell. If variability in P*_IIA_*-*gfp* expression were simply the result of cell-to-cell differences in overall macromolecular synthesis, its level should be highly correlated with P*_Hy_*-*mCherry*, whose expression is independent of the proteins involved in sporulation. The low correlation coefficient observed between the two reporters, combined with the previously
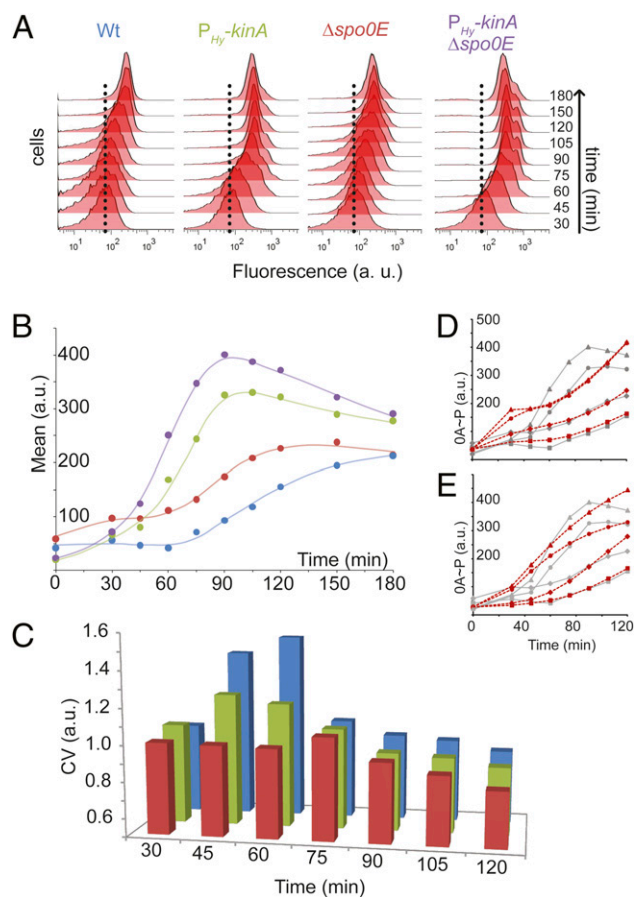

Fig. 5. Effect of phosphate flux on 0A activity and prediction of 0A~P accumulation by computational modeling. (*A*) FACS analysis of the effect of KinA and 0E on P*_IIA_*-*gfp* expression. As in Fig. 4*B* except that samples were collected every 15 min as indicated. Cell distributions were determined for strains harboring *amyE*::P*_IIA_*-*gfp*. The strains were otherwise wild type (wt), mutant for *spo0E* (Δ*spo0E*), overexpressing *kinA* (*kinA*::P*_Hy_*-*kinA*), or mutant for *spo0E* and overexpressing *kinA* (*kinA*::P*_Hy_*-*kinA* ; Δ*spo0E*). Induction was performed by adding 1 mM IPTG (final concentration) at the time of suspension (time 0). Dotted lines were arbitrarily placed at 70 a.u. to serve as a reference to highlight the shifting of the peak numbers of fluorescent cells. (*B*) The increase in mean fluorescence is nonlinear and is delayed by 0E activity. From data collected during FACS analysis (*A*), mean fluorescence was calculated for each distribution diagram and plotted as a function of time. Blue symbols correspond to wild type, red to Δ*spo0E*, green to *kinA*::P*_Hy_*-*kinA*, and purple to *kinA*::P*_Hy_*-*kinA*, Δ*spo0E*. (*C*) 0E and variations in phosphate flux contribute to heterogeneity in P*_IIA_*-gfp expression. From data collected during FACS analysis (*A*), the CV (defined as the ratio of the distribution SD to its mean) was calculated for each distribution diagram and plotted as a function of time. Blue symbols correspond to wild type, red to Δ*spo0E*, and green to *kinA*::P*_Hy_*-*kinA*. (*D* and *E*) Predicted kinetics of 0A~P accumulation calculated to fit to the mean fluorescence in wt (■), Δ*spo0E* (◆), *kinA*::P*_Hy_*-*kinA* (●), and *kinA*::P*_Hy_*-*kinA*; Δ*spo0E* (▲), assuming that mean fluorescence was proportional to the level of 0A~P. Gray curves are experimental data (*B*; mean fluorescence), and dotted red curves are predictions. Model 1 (*D*) assumes a linear increase of all relay components and model 2 (*E*) assumes that + feedback loops driven by 0A~P govern increase in KinA, 0F, 0B, and 0A.

reported low intrinsic noise of this promoter (10), shows instead that the pathway governing the accumulation of 0A~P is likely responsible for the variability and hence likely to be noisy.

A slightly different result was observed with another 0A~P-controlled promoter P*_IIE_* (that of *spoIIE*). Expression of P*_IIE_*-*gfp* commenced later than for P*_IIA_*-*gfp* and exhibited a broad distribution, which then coalesced into a high-level expression peak with a tail (120 min) (Fig. 4*B*). The presence of multiple putative binding sequences for 0A in *spoIIE* promoter raises the possi-

SYSTEMS BIOLOGY

bility that in this case cooperative interactions among 0A~P bound molecules imparted a heavy-tailed, non-Gaussian distribution of expression levels. Nevertheless, this long-tail distribution does not constitute bona fide bimodality.

Phosphate Flux Governs the Rate and Timing of 0A~P Activation. Next, we took advantage of flow cytometry to analyze the role of phosphate flux in 0A~P activity by monitoring the effect of a *spo0E* mutation and overexpression of *kinA* on P$_{IIA}$-*gfp* expression. Fig. 5*A* shows the flow cytometry tracings, and Fig. 5*B* shows corresponding mean fluorescence for each time point so that the changes can be compared over time. We noticed that the increase in 0A~P levels was nonuniform, with a slow stage lasting approximately 1 h, followed by a stage with significantly higher accumulation rate. Additionally, the absence of the 0E phosphatase increased the expression of P$_{IIA}$-*gfp*, thereby shortening the accumulation stage. Thus, 0E phosphatase in effect creates a delay for the induction of P$_{IIA}$-*gfp*. Because after the initial slow stage the rate of GFP accumulation (the slope of the curve in Fig. 5*B*) was largely the same in the 0E mutant as in the wild type, it seems that once the concentration of 0A~P had started to increase rapidly the contribution of the 0E phosphatase became negligible. In contrast, overproduction of KinA significantly accelerated, after a short delay, the rate of GFP accumulation. Finally, when KinA was overproduced in a *spo0E* mutant, the rate of GFP accumulation was accelerated but with less of a delay. We conclude that the 0E negative feedback loop is a timer that delays a stage of fast 0A~P induction, whereas the rate of increase in 0A~P activity is largely determined by phosphate flux.

We also determined the CV for the distribution of 0A~P among cells in the population (Fig. 5*C*). CV has been used to characterize noise in gene expression (18, 19). We observed that in the wild type the distribution heterogeneity reached a maximum in approximately 45–60 min. Interestingly, both overexpressing *kinA* and deleting *0E* caused heterogeneity to decrease significantly (the CV was 40–60% higher in the wild type than in the overexpression strain and the mutant). From this, we conclude that both 0E and variations in phosphate flux contribute to noise in 0A~P accumulation.

Computational Model Demands an Increase in the Amount of Relay Proteins During Sporulation. Finally, we built a computational model for the 0A regulatory network to simulate the kinetics of 0A~P accumulation (assuming that 0A~P was proportional to the mean fluorescence). Modeling was performed using, separately, ordinary differential equations and stochastic equations based on Gillespie's algorithm (20). To build the model, we used equations describing transcription, translation, protein, and RNA degradation for KinA, 0F, 0B, 0E, and 0A, plus important phosphorylation reactions of the relay (KinA→ 0F, 0F→ 0B, 0B→ 0A), the 0A autoregulatory loop, the dephosphorylation of 0A~P by 0E, and the induction of *spo0E* by 0A~P. When biochemical parameters were unknown, we relied on previously reported generic parameters (*Appendix S1*). On the basis of aforementioned results, AbrB and σ^H were left out of the model.

In modeling we noticed that to fit the experimental results, we needed to take into account the fact that 0E was overpowered after the initial delay (Fig. 5*B*). To account for the fast accumulation of 0A~P after 60 min, we had to introduce a significant increase in the amount of KinA. For this, we invoked a linear increase in the rate of *kinA* transcription, but then other components of the relay became rate limiting, and it proved necessary to increase 0A, 0B, and 0F levels as well. Thus, we introduced similar linear increases in the accumulation of KinA, 0B, 0F, and 0A and optimized the starting point and rates of the increase. The best fit to the experimental data, for both the wild type and the *0E* mutant, was achieved when the relay proteins started to increase at approximately 30 min at a rate of

approximately 300% per hour (model 1; Fig. 5*D*). We also attempted to simulate 0A~P accumulation by invoking positive feedback loops in all four proteins instead of a linear increase either on the transcriptional or translational level. To avoid combinatorial fitting of parameters, we assumed the same feedback function for all loops and optimized the feedback strength and sharpness (model 2; Fig. 5*E*). Both models fit the experimental data reasonably well. It should be noted that although in model 2 the feedback loops are activated only after 0A~P reaches a certain threshold, the network does not reach a new stable steady state after that point. Instead, as in the experimental data, the increasing activity of feedback loops ensures just-in-time increases in the concentrations of the relay proteins for a continuous increase in the 0A~P level.

Discussion

Our investigation makes four contributions. First, we provide insight into the function of the feedback loops that govern the synthesis and phosphorylation of 0A. Second, we show that activation of 0A~P occurs in a broadly heterogeneous manner, which, as we propose, arises from noise in flux of phosphate through the relay. Third, we find that 0A activity (0A~P levels) increases in a nonlinear fashion, with an initial slow phase followed by a rapid phase. Fourth, we present time-resolved, computational models predicting an increase in the amount of relay proteins during sporulation that could explain the observed pattern of 0A~P accumulation.

Function of the Feedback Loops. Synthesis and phosphorylation of 0A~P is influenced by four feedback loops, which we interpret as follows (Fig. 1*B* and Fig. S4):

(*i*) The 0A~P⊣ AbrB→ σ^H→ 0A loop is an early switch that is turned on before the period of 0A~P accumulation. Its activation is a prerequisite for 0A~P accumulation, but it does not contribute significantly to the kinetics of 0A~P accumulation.

(*ii*) The 0A~P→ 0A and 0A~P→ 0F loops are just-in-time circuits that maintain adequate levels of 0A and 0F as 0A~P levels rise, ensuring that neither protein becomes rate limiting. Because 0A accumulates to up to 20,000 molecules per cell (Fig. S1), it would be wasteful to produce a full amount of 0A molecules before they need to be phosphorylated. In the case of 0F, we have shown that it is rate limiting for sporulation at low concentrations and becomes inhibitory at high levels. Therefore, the 0A~P→ 0F loop calibrates the amount of 0F needed as 0A~P levels rise.

(*iii*) Finally, 0A~P→ 0E⊣ 0A~P is a negative feedback loop that imposes a delay before 0A~P levels begin to significantly rise. Interestingly, the loop does not influence the rate of 0A~P increase after the delay.

Broadly Heterogeneous Activation of 0A. It has been assumed and reported that 0A activation is bimodal, with one or more of the positive feedback loops creating a bistable switch (10, 21). Instead, we find that 0A activity varies greatly from cell to cell and that none of the known loops serve as bistable switches (Fig. S4*A*). What is then the basis for the heterogeneity? We favor the idea that it is generated by noise in the flux of phosphates through the relay. This noise could arise *stricto sensu* from the core components of the relay (KinA, 0F, 0B, 0A) or from accessory proteins, such as the phosphatases (Rap and 0E families) known to drain phosphates from the relay (22, 23). Indeed, it is tempting to imagine that the selection for a four-component relay instead of the related, classic two-component system, may

have been [apart from integrating environmental signals (23)] a way to generate noise.

A Computational Model for 0A Activation. The main conclusions from the FACS data are (*i*) 0E delays the time at which 0A~P levels start to increase significantly, and (*ii*) after the delay, the subsequent rate of the 0A~P accumulation is primarily governed by phosphate flux and not by 0E. We attempted to describe this pattern of 0A activation by creating a computational model. A striking conclusion from the modeling simulations was a requirement to significantly increase the amount of relay proteins at some time point after the beginning of sporulation. A slightly better fit for the rise in 0A~P levels was achieved when we assumed that the rates of accumulation of KinA, 0A, 0B, and 0F accelerate owing to positive feedback (model 2). Because no such loops operating at the transcriptional level are known for *kinA* (recall that σ^H, which drives *kinA* transcription, is not rate limiting) and *spo0B*, thus the model, if true, would imply the existence of an unknown posttranscriptional mechanism to stimulate the accumulation of KinA and 0B.

Biologic Significance. What is the biologic significance that 0A activation is broadly heterogeneous and primarily controlled by the phosphate flux? We suggest that one of the major functions of the phosphorelay, in addition to integrating environmental signals, is to create asynchrony in the time of entry into sporulation. Sporulation requires a high threshold concentration of 0A~P, and only cells attaining this threshold are able to proceed through morphogenesis (Fig. S4). In fact, not all cells in the population reach this threshold and succeed in forming spores. Indeed, and as we have shown, artificially increasing phosphate flux decreases asynchrony and increases the proportion of spore-forming cells. Spore formation and the subsequent process of germination are costly in time and energy. Thus, asynchrony helps to ensure that all cells do not commit to spore formation at once, an advantageous strategy given the vicissitudes of the environment.

In contrast to other systems that generate cell population heterogeneity (such as genetic competence), the rate-limiting factor in the 0A network is not the transcription factor concentration but phosphate flux. This ensures that *en route* to committing to sporulation *B. subtilis* constantly monitors environmental conditions through the persistence of this flux. If conditions improve, KinA activity drops and phosphatases, such as 0E, quickly drain phosphate from the network. Thus, 0E plays the role of a persistence indicator, delaying 0A~P accumulation and allowing the majority of the cells to enter sporulation only if adverse environmental conditions persist.

Finally, heterogeneity in 0A~P levels has additional advantages for cells growing to high cell density on surfaces, conditions under which cells exhibit cannibalism—itself a delaying tactic for spore formation—and biofilm formation. As noted previously, activation of some target genes, such as those involved in cannibalism and biofilm formation, requires a low threshold concentration of 0A~P. Thus, variation in the rates of accumulation of 0A~P ensures that cells exhibit a variety of behaviors.

Materials and Methods

Media, culture and cloning procedures, and β-galactosidase assay were performed as described previously (24, 25). Immunoblot analyses were performed as described previously (24) using a 10^{-4} dilution for primary antibody and 2.10^{-4} dilution of secondary goat anti-rabbit IgG-HRP conjugate (Bio-Rad). Plasmid and strain construction are described in *SI Materials and Methods*. For assaying sporulation by fluorescence microscopy, membranes were stained using Mito-Tracker Green FM (Molecular Probes) following a previously described procedure (24), and cell counting was performed using the Metamorph software suite.

For the flow cytometry (FACS) experiment, cell samples were suspended in an equivalent volume of ice-cold PBS buffer and analyzed using a BD LSR II flow cytometer (BD Biosciences) with 30,000 events recorded for each sample. Data were collected with FACS Diva software (BD Biosciences) and analyzed with FlowJo 8.5.2 and the FCA 2.2 flow cytometry analysis package for Matlab. Stochastic computational simulations were performed using the program DIZZY (26). Kinetics of 0A~P accumulation prediction were obtained by averaging 5,000 individual stochastic simulations. The results of computational modeling were compared with the experimental data by minimizing the rmsd between all simulated and observed time points (from 0 to 120 min) in wild type and in all mutants (see *Appendix S1* for details).

1. Chai Y, Chu F, Kolter R, Losick R (2008) Bistability and biofilm formation in *Bacillus subtilis*. *Mol Microbiol* 67:254–263.
2. Dubnau D, Losick R (2006) Bistability in bacteria. *Mol Microbiol* 61:564–572.
3. Kearns DB, Losick R (2005) Cell population heterogeneity during growth of *Bacillus subtilis*. *Genes Dev* 19:3083–3094.
4. Maamar H, Raj A, Dubnau D (2007) Noise in gene expression determines cell fate in *Bacillus subtilis*. *Science* 317:526–529.
5. Fujita M, Losick R (2005) Evidence that entry into sporulation in *Bacillus subtilis* is governed by a gradual increase in the level and activity of the master regulator Spo0A. *Genes Dev* 19:2236–2244.
6. Burbulys D, Trach KA, Hoch JA (1991) Initiation of sporulation in *B. subtilis* is controlled by a multicomponent phosphorelay. *Cell* 64:545–552.
7. Fujita M, González-Pastor JE, Losick R (2005) High- and low-threshold genes in the Spo0A regulon of *Bacillus subtilis*. *J Bacteriol* 187:1357–1368.
8. Phillips ZE, Strauch MA (2002) *Bacillus subtilis* sporulation and stationary phase gene expression. *Cell Mol Life Sci* 59:392–402.
9. Chung JD, Stephanopoulos G, Ireton K, Grossman AD (1994) Gene expression in single cells of *Bacillus subtilis*: Evidence that a threshold mechanism controls the initiation of sporulation. *J Bacteriol* 176:1977–1984.
10. Veening JW, Hamoen LW, Kuipers OP (2005) Phosphatases modulate the bistable sporulation gene expression pattern in *Bacillus subtilis*. *Mol Microbiol* 56:1481–1494.
11. Chibazakura T, Kawamura F, Takahashi H (1991) Differential regulation of *spo0A* transcription in *Bacillus subtilis*: Glucose represses promoter switching at the initiation of sporulation. *J Bacteriol* 173:2625–2632.
12. Banse AV, Chastanet A, Rahn-Lee L, Hobbs EC, Losick R (2008) Parallel pathways of repression and antirepression governing the transition to stationary phase in *Bacillus subtilis*. *Proc Natl Acad Sci USA* 105:15547–15552.
13. O'Reilly M, Devine KM (1997) Expression of AbrB, a transition state regulator from *Bacillus subtilis*, is growth phase dependent in a manner resembling that of Fis, the nucleoid binding protein from *Escherichia coli*. *J Bacteriol* 179:522–529.

14. Asai K, Kawamura F, Yoshikawa H, Takahashi H (1995) Expression of *kinA* and accumulation of sigma H at the onset of sporulation in *Bacillus subtilis*. *J Bacteriol* 177:6679–6683.
15. Healy J, Weir J, Smith I, Losick R (1991) Post-transcriptional control of a sporulation regulatory gene encoding transcription factor sigma H in *Bacillus subtilis*. *Mol Microbiol* 5:477–487.
16. Jiang M, Shao W, Perego M, Hoch JA (2000) Multiple histidine kinases regulate entry into stationary phase and sporulation in *Bacillus subtilis*. *Mol Microbiol* 38:535–542.
17. Grimshaw CE, et al. (1998) Synergistic kinetic interactions between components of the phosphorelay controlling sporulation in *Bacillus subtilis*. *Biochemistry* 37:1365–1375.
18. Newman JR, et al. (2006) Single-cell proteomic analysis of *S. cerevisiae* reveals the architecture of biological noise. *Nature* 441:840–846.
19. Raj A, van Oudenaarden A (2008) Nature, nurture, or chance: Stochastic gene expression and its consequences. *Cell* 135:216–226.
20. Gillespie DT (1977) Exact stochastic simulation of coupled chemical reactions. *J Phys Chem* 81:2340–2361.
21. Morohashi M, et al. (2007) Model-based definition of population heterogeneity and its effects on metabolism in sporulating *Bacillus subtilis*. *J Biochem* 142:183–191.
22. Perego M (2001) A new family of aspartyl phosphate phosphatases targeting the sporulation transcription factor Spo0A of *Bacillus subtilis*. *Mol Microbiol* 42:133–143.
23. Perego M, et al. (1994) Multiple protein-aspartate phosphatases provide a mechanism for the integration of diverse signals in the control of development in *B. subtilis*. *Cell* 79:1047–1055.
24. Chastanet A, Losick R (2007) Engulfment during sporulation in *Bacillus subtilis* is governed by a multi-protein complex containing tandemly acting autolysins. *Mol Microbiol* 64:139–152.
25. Sterlini JM, Mandelstam J (1969) Commitment to sporulation in *Bacillus subtilis* and its relationship to development of actinomycin resistance. *Biochem J* 113:29–37.
26. Ramsey S, Orrell D, Bolouri H (2005) Dizzy: Stochastic simulation of large-scale genetic regulatory networks. *J Bioinform Comput Biol* 3:415–436.

SYSTEMS BIOLOGY